

Mining MOOC Clickstreams: On the Relationship Between Learner Video-Watching Behavior and Performance

Christopher G. Brinton, Swapna Buccapatnam, Mung Chiang, and H. Vincent Poor

Department of Electrical Engineering
Princeton University, Princeton, NJ 08544
{cbrinton, swapnab, chiangm, poor}@princeton.edu

ABSTRACT

We study student behavior and performance in two Massive Open Online Courses (MOOCs). In doing so, we present two frameworks by which video-watching clickstreams can be represented: one based on the sequence of events created, and another on the sequence of positions visited. With the event-based framework, we extract recurring subsequences of student behavior, which contain fundamental characteristics such as reflecting (*i.e.*, repeatedly playing and pausing) and revising (*i.e.*, plays and skip backs). We find that some of these behaviors are significantly associated with whether a user will be Correct on First Attempt (CFA) or not in answering quiz questions. With the position-based framework, we then devise models for performance. In evaluating these through CFA prediction, we find that three of them can substantially improve prediction quality in terms of accuracy and F1, which underlines the ability to relate behavior to performance. Since our prediction considers videos individually, these benefits also suggest that our models are useful in situations where there is limited training data, *e.g.*, for early detection or in short courses.

Keywords

Clickstream Data, Video-Watching Behavior, Motif Identification, Data Mining, Performance Prediction, MOOC

1. INTRODUCTION

Over the past decade, technology advances have been influencing the ways we can learn. One such innovation has been the Massive Open Online Course (MOOC), with platforms such as Coursera, edX, and Udacity offering MOOCs that have reached hundreds of thousands of students within single sessions. The low completion rates in these courses, caused in part by small teacher-to-student ratios and the asynchronous nature of interaction, has ignited research interest in data mining and (human) learning theory [5].

A standard MOOC contains three different learning modes for students: video lectures, assessments (*e.g.*, in-video quizzes,

homework, and exams), and social networking [8]. Most platforms track student interaction with these forms of learning. For video, this information includes clickstream events, which are generated each time a learner interacts with a video. For assessments, the specific responses to individual questions are tracked, and for the discussion forums, the sequence of posts and comments are stored. This type of data has motivated a number of recent studies focused on understanding how MOOC users learn (*e.g.*, [11, 17, 7]).

What remains understudied, however, is the *relationship* between these learning modes. In particular, is it possible to associate a student's *behavior* with his/her *performance* in a MOOC? This question has far-reaching implications to methods for improving low completion rates, such as personalized content delivery [8] and instructor analytics [20].

Our work is motivated by this fundamental question. In our investigation, we focus on the video-watching behavior of MOOC students, where users spend the majority of their time learning [11]. These videos are typically equipped with quiz questions, which serve as immediate feedback of the knowledge a student gained from the content in the video. In relating behavior to performance, then, we can consider the clickstreams generated by a user in watching the video associated with a particular quiz, and whether the user was Correct on First Attempt (CFA) or not in answering the given question.

In our investigation, we formalize different ways in which video-watching clickstreams can be represented as compact sequences, and apply the frameworks we develop to meet two objectives:

- *O1. Identifying recurring behaviors of learners*, such as revising content or skipping forward repeatedly.
- *O2. Assessing the impact of behavior on performance*, such as those patterns identified in O1, and the specific positions visited in each video.

In doing so, we employ two datasets coming from two different MOOCs, which contain (after filtering) 315K and 416K clickstream event logs corresponding to 26K and 36K first-attempt quiz submissions.

Previous work [17] has focused on the sequence of *events* (*e.g.*, play, pause, skip forward) generated by MOOC users in watching videos. In studying O1 and O2, we identify two additional factors that are important to capture: the *positions* in the video that a user visited, and the *duration / length* of time between the events and positions. In particular, we first develop an event-based framework to represent clickstreams (Sec. 2), which captures event types and their

Permission to make digital or hard copies of all or part of this work for personal or classroom use is granted without fee provided that copies are not made or distributed for profit or commercial advantage and that copies bear this notice and the full citation on the first page. To copy otherwise, to republish, to post on servers or to redistribute to lists, requires prior specific permission and/or a fee.

Copyright 20XX ACM X-XXXXX-XX-X/XX/XX ...\$15.00.

Dataset	Lectures	Lecture Videos	Video Length (min) avg. (s.d.)	Quizzes	Users	Clickstream Events	User-Video Pairs	CFA Score avg. (s.d.)
‘FMB’	20	92	16.9 (5.96)	92	3770	314,632	26,250	0.663 (0.473)
‘NI’	6	115	5.44 (2.17)	69	2680	416,214	36,464	0.750 (0.433)

Figure 1: Basic information on the two datasets. The values in the right column are the final numbers after data filtering.

lengths. Leveraging this framework, we find recurring subsequence *motifs* in our two datasets, for O1 (Sec. 3), as well as a significant difference in the presence of certain motifs across CFA and non-CFA sequences, for O2. For example, we find that a series of behaviors are indicative of students reflecting on material, and are significantly associated with the CFA sequences in one of the courses. As another example, we identify motifs that are consistent with rapid-paced skimming through the material, and reveal that these are discriminatory in favor of non-CFA in both courses. Incorporating the lengths in addition to the events was essential to these findings, because motif extraction with the events alone does not reveal these insights.

In investigating O2, we also seek to develop models for knowledge gained based on user clicks in a video. The quality of such a model can be evaluated by considering its ability to generalize to incoming samples through *prediction*. To this end, we will study CFA prediction, which is an important area of research in its own right because it can, for example, help in early detection of struggling and advanced students, and of easy and difficult material [6].

In seeking appropriate models for student performance, we find that while some behavioral patterns of the motifs are significantly associated with performance, their supports and the resulting success estimates are likely not sufficient for prediction. As a result, we propose a second behavioral representation, which uses the sequence of positions visited in a video (Sec. 4). Moreover, in contrast to training over a long course duration as in [6, 13], we consider CFA prediction on a *per-video* basis, in order to quantify the benefit obtained by the positions in each individual video. We evaluate four different models based on this framework (Sec. 5), and find that three of them obtain substantial improvements in prediction when compared to a baseline that does not use click information. This underscores the ability to relate clicks to knowledge gained, and shows that behavioral information is useful in situations where multiple videos are not be available, *e.g.*, in short courses or for detection early in a course.

Summary of contribution. Compared with other work (Sec. 6), we make three contributions. First, we present two novel frameworks for representing clickstream sequences, which we are useful in identifying recurring behavioral patterns and for CFA prediction. Second, we extract recurring subsequences from user clicks using motif identification schemes, and associate these fundamental behaviors with student performance. Third, we show how user click behavior can be used to enhance prediction on a per-video basis.

2. DATASETS AND CLICKSTREAMS

In this section, we describe our datasets, and present our first sequence specification based on events and lengths.

2.1 Two Courses

Our datasets come from two different courses we have instructed on Coursera: *Networks: Friends, Money, and Bytes* (‘FMB’) and *Networks Illustrated: Principles Without Cal-*

culus (‘NI’).¹ Each of these courses teach networking, but ‘FMB’ delves into mathematical specifics, whereas ‘NI’ is meant as an introduction to the subject (see [8] for details). We obtained two types of data from each course: video-watching clickstreams, which log user interaction with the video player, and quiz submission information.

Course format. The course formats are summarized in Fig. 1. Each contains a series of lectures, in turn comprised of a set of videos. ‘FMB’ is a longer course, with 20 lectures, whereas ‘NI’ only has 6. ‘NI’ had more, shorter-length videos, with a total of 115 and an average (avg.) length of 5.4 min per video, whereas ‘FMB’ has a total of 93 with an avg. length of 16.9 min.

Each course has in-video quizzes, in the form of single multiple choice questions with four choices each. For ‘FMB’, there was one question at the end of each video. For ‘NI’, each of the 69 questions was associated with anywhere from 1 to 4 videos. As a result, in mapping videos to quizzes, we will refer to “video X” as the contiguous set of videos occurring after question $X - 1$ and before question X .

User-Video Pairs. Given our goal of relating user behavior to performance, we extract User-Video (UV) Pairs from the data, which consisting of two sets of information:

- *Video-watching trajectory:* The set of clickstream logs (events) for the user in the video.
- *CFA result:* Whether the user was Correct on First Attempt (CFA) or not for the corresponding quiz.

In total, there were 122.5K UV Pairs for ‘FMB’, with 566K click events. For ‘NI’, these numbers were 149K and 882K, respectively. After removing any UV Pair that had at least one `null`, stall or error recorded, we were left with the numbers given in Fig. 1 for each course. The avg. CFA score across the UV Pairs was 0.663 for ‘FMB’ (standard deviation (s.d.) = 0.47), and 0.750 for ‘NI’ (s.d. = 0.43).

2.2 Clickstream Events

2.2.1 Our nomenclature for events

Clickstream logs are generated as one of four types: **play**, **pause**, **ratechange**, and **skip**. Each time one of these events is fired, a data entry is recorded that specifies the user and video IDs, event type, playback position, playback speed, and UNIX timestamp for the event.

Formally, let E_i denote the i th click event that occurs while a user is watching a video. We write $E_i = \langle e_i, p_i, t_i, s_i, r_i \rangle$, where e_i is the type of the i th click, p_i is the video position (in sec) right after E_i is fired, t_i is the UNIX time (in sec) at which E_i was fired, s_i is the state of the video player – either **playing** or **paused** – as a result of E_i , and r_i is the playback rate (*i.e.*, speed) of the video player resulting from this event. The logs are sequenced chronologically for a UV Pair, *i.e.*, $t_1 < t_2 < \dots$. Based on these E_i , we define the following events:

Play (PI): A play event begins at the time when a click event E_i is made for which the state s_i is **playing**, and

¹www.coursera.org/course/{friendsmoneybytes,ni}

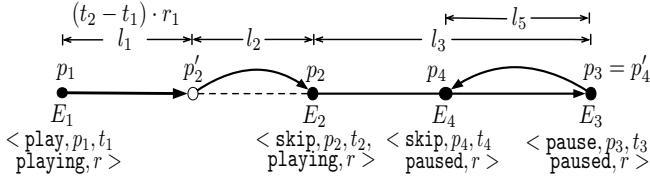


Figure 2: Illustration of a sequence of clicks E_1 to E_4 on a video, where the horizontal axis denotes the video length. The length parameter l_j for the 4 (of 5) resultant events that have this property are depicted above the diagram.

lasts until the next click E_{i+1} . It occurs for a duration $d = t_{i+1} - t_i$ and has a length $l = p_{i+1} - p_i$.

Pause (Pa): A pause event is defined in the same way as a play event, except it is for which the state s_i is **paused**, and does not have any length by definition.

Skip back (Sb): A skip back (*i.e.*, rewind) event occurs when E_i is a skip and $p'_i > p_i$, where p'_i is the position of the video player immediately before the skip. If $s_{i-1} = \text{playing}$, then $p'_i = p_{i-1} + (t_i - t_{i-1}) \cdot r_{i-1}$; if $s_{i-1} = \text{paused}$, then $p'_i = p_{i-1}$. The length of the skip is $l = |p_i - p'_i|$, and there is no associated duration.

Skip forward (Sf): A skip forward (*i.e.*, fast forward) event is defined as Sb, except it captures the case where $p_i > p'_i$.

Ratechange fast (Rf): This event occurs when E_i is a ratechange and the rate $r_i > 1.0$.² There is no d or l .

Ratechange slow (Rs): This occurs when e_i is ratechange and $r_i < 1$, again with no duration or length.

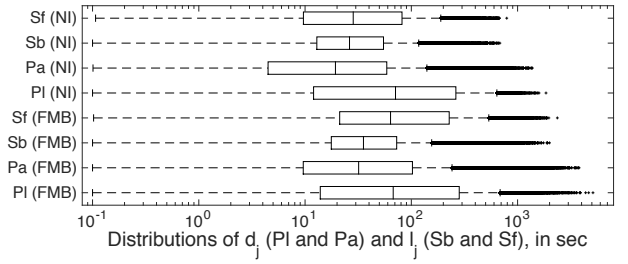
Ratechange default (Rd): This occurs when e_i is ratechange and $r_i = 1$, *i.e.*, returning to the default.

The sequence of events for a UV Pair then becomes $\hat{e}_1, \hat{e}_2, \dots$ for $\hat{e}_j \in \mathcal{E} = \{\text{Pl, Pa, Sb, ...}\}$, $|\mathcal{E}| = 8$. Each \hat{e}_j may have an associated duration d_j and/or length l_j . Fig. 2 shows a schematic to illustrate this; the clickstream logs here would generate: Pl, with $l_1 = (t_2 - t_1) \cdot r$ and $d_1 = t_2 - t_1$; Sf, with $l_2 = p_2 - p'_2$; Pl, with $l_3 = p_3 - p_2$ and $d_3 = t_3 - t_2$; Pa, with $d_4 = t_4 - t_3$; Sb, with $l_5 = p'_4 - p_4$. Note that we are inserting Pl and Pa events in-between other events, to incorporate the state of the video player during those times. This critical information is not captured through only the events in the raw data, and has been neglected in other work (*e.g.*, in [17]).

Denosing clickstreams. In order to remove noise associated with unintentional user behavior, we handle two cases of events separately:

Combining events: We combine repeated, sequential events that occur within a short duration (5 sec) of one another, since this indicates that the user was adjusting to a final state. For example, if a series of Sf or Sb events occur within a few seconds of each other, then likely the user was simply looking for the final position, so it should be treated as a single skip to that final location. Similarly, if a series of Rf or Rs events occur in close proximity, then the user was likely in the process of adjusting the rate to the final value. Formally, if there is a sequence of clicks $E_i, E_{i+1}, \dots, E_{i+k}$ for which $\hat{e}_i = \hat{e}_{i+1} = \dots = \hat{e}_{i+k}$ and $t_{i+1} - t_i < 5 \forall i$, then we use $E'_i = \langle e_i, p_{i+k}, t_{i+k}, s_{i+k}, r_{i+k} \rangle$ in place of $E_i, E_{i+1}, \dots, E_{i+k}$. **Discounting intervals:** There are two cases in which **play** and **pause** events will not be inserted between E_i and E_{i+1} . First is if E_i and E_{i+1} occur on two different videos; in this

²The default player speed is 1.0, and users can vary this between 0.5 and 2.0, in increments of 0.25.



(a) Boxplots of the distributions for each dataset.

Dataset	Event	Size	Frac	Q_1	Q_2	Q_3
'FMB'	Pl	112.7K	53%	13.9	67.5	282.4
	Pa	51.2K	24%	9.6	31.9	102.4
	Sb	29.4K	14%	17.7	35.4	72.7
	Sf	18.2K	8.6%	21.2	63.7	227.2
'NI'	Pl	103.5K	58%	12.0	71.0	262.6
	Pa	46.4K	26%	4.5	19.3	58.8
	Sb	17.8K	10%	12.9	26.2	54.7
	Sf	10.7K	6.0%	9.6	28.4	81.7

(b) Tabulated statistics for the distributions.

Figure 3: Distribution of the lengths for four events across both 'NI' and 'FMB'. For Pl and Pa, this represents the time elapsed before the next event, and for Sb and Sf, this is the distance of the skip.

case, there is no continuity between i and $i + 1$, since the user must have exited the first video and then opened the second one. As a result, the Pl or Pa that would have been added in-between these events will not be captured. The second case occurs when the duration d is extremely long between between E_i and E_{i+1} . In this case, it is likely that the user was engaging in some off-task behavior during this time. If $s_i = \text{paused}$, the threshold is set to 20 min (as in [22] for web inactivity); if $s_i = \text{play}$, then the threshold is set to the length of the video.

2.2.2 Event lengths

We now look to discretize the length l_j and duration d_j of the events for comparative purposes. To this end, Fig. 3(a) gives the boxplots of the event distributions from each course. d_j for Pl and Pa is shown, and we depict l_j for Sb and Sf. Also, in these plots, we show only values that are at least 0.1 sec. Basic statistics of each distribution are also given in Fig. 3(b); specifically, the three quartiles Q_1 , Q_2 , and Q_3 are shown,³ as are the number of events for each distribution (Size) and the respective fractions (Frac).

Overall, we make three main observations in comparing the distributions. In each case, we employed a Wilcoxon Rank Sum (WRS) [16] test for the null hypothesis that there was no difference between the distributions for each dataset overall, and report the p-values (p) from those tests:⁴

(1) *'FMB' has longer events:* The distributions for each event are shifted to the right for 'FMB' relative to those for 'NI', meaning that 'FMB' tends to have longer events. In each of the four cases (Pl, Pa, Sb, and Sf), the p-values (p) were highly significant ($p \approx 0$). This highlights that event durations can be dependent on the content. The fact that the 'FMB' content is more difficult may explain why Pa

³By definition, quartiles separate data in increments of 25%.

⁴We use the WRS test because Shapiro-Wilk tests detected significant departures from normality for each of the distributions.

tends to be longer. But then we would expect the length of P1 to be *shorter*, in order for the students to process material in shorter bits, which is not the case.

(2) *Sf is longer than Sb*: The distribution of skip forward is shifted to the right relative to skip back for both ‘FMB’ and ‘NI’ ($p < 1E-6$). This indicates that when students skip forward, they tend to pass more material than they revise when skipping back. The fraction of Sf events is also roughly half the fraction of Sb events for both datasets, *i.e.*, skipping back is more common.

(3) *Pl is longer than Pa*: The distributions for play and pause in both datasets indicate that users tend to stay in the **playing** state longer than **paused** ($p \approx 0$). This effect is stronger in the case of ‘NI’ (*e.g.*, the ratio of the medians is 3.68 for ‘NI’, and only 2.11 for ‘FMB’). Again, this is consistent with the fact that the ‘FMB’ material is more difficult, which would tend to cause students to pause longer relative to play duration.

Event intervals. Clearly, l_j and d_j can vary substantially between events and datasets. To account for this relative variation, we will use the four intervals in-between the three quartiles for each event (given in Fig. 3(b)) to discretize the lengths.⁵ We specify three cases:

(1) $\hat{e}_j \in \{\text{Sb}, \text{Sf}\}$: When the event is a skip, we map it to $\langle \hat{e}_j, q_j \rangle$, where $q_j \in \{1, 2, 3, 4\}$ is chosen such that $l_j \in [Q_{q_j-1}, Q_{q_j}]$, with $Q_0 = 0$ and $Q_4 = \infty$. For example, suppose that event E_i is such that $\hat{e}_j = \text{Sb}$ and $l_j = 20$ sec. In either course, this would be mapped to **Sb2**.

(2) $\hat{e}_j = \text{Pa}$: In this case, the mapping works the same as the previous, except q_j is chosen based on d_j instead.

(3) $\hat{e}_j = \text{Pl}$: Two long duration play events could still have different qualitative interpretations.⁶ To account for this, when $\hat{e}_j = \text{Pl}$, we map it to $\langle \hat{e}_j, q_{j,1} \hat{e}_j, q_{j,2} \dots \hat{e}_j, q_{j,n} \rangle$, where $q_{j,k} \in \{1, 2, 3\}$ for $k = 1, \dots, n$ is chosen according to:

$$q_{i,k} = \begin{cases} 3, & d_j - \delta_{j,k} > Q_3 \\ \arg \max_{q_{j,n}} (d_j - \delta_{j,n} \leq Q_{q_{j,n}}), & \text{otherwise,} \end{cases}$$

with $\delta_{j,k} = \sum_{k'=1}^{k-1} Q_{q_{j,k'}}$. For example, suppose an event is P1 with $d_j = 550$ sec. For the quartiles in ‘NI’, this would be mapped to **P13 P13 P12**.

2.2.3 Event-type sequence specification

Let $\mathcal{S} = \{\text{P11}, \text{P12}, \text{P13}, \text{Pa1}, \dots, \text{Pa4}, \text{Sb1}, \dots, \text{Sb4}, \text{Sf1}, \dots, \text{Sf4}, \text{Rf}, \text{Rs}, \text{Rd}\}$, with $|\mathcal{S}| = 18$. For each UV Pair, we encode the clickstream $\log E_1, \dots, E_n$ as $S = (s_1, s_2, \dots, s_n)$ where each $s_j \in \mathcal{S}$ is chosen according to the specifications in Sec. 2.2.2. As we will see in Sec. 3, using an alphabet that incorporates both event types and lengths allows us to obtain insights that are difficult to glean with events alone.

For purpose of comparison, we will refer to a length of 1 as “short,” 2 as “medium,” 3 as “medium-long,” and 4 as “long.”

3. MOTIFS OF VIDEO-WATCHING

Using the event-type specification, we identify short, recurring sub-sequences within user behavior, *i.e.*, behavioral

motifs. As we will see in Sec. 3.2, these motifs capture fundamental video watching characteristics such as reflecting on or revising material. We will also see that some of these motifs are significantly associated with performance.

3.1 Motif Extraction

In order to find the motifs in our datasets, we make use of a well-known, open-source software package called MEME Suite [3]. MEME has been widely applied in bioinformatics, for motif identification in sequences of nucleotides and amino acids. We find MEME to be applicable to our setting as well. **MEME algorithm.** The algorithm underlying MEME is based on a probabilistic mixture model, where the key assumption is that each subsequence is generated by one of two components: a position-*dependent* motif model, or a position-*independent* background model. Under the motif model, each position j in a motif is described by a multinomial distribution, which specifies the probability of each character occurring at occurring position j . On the other hand, the background model is a multinomial distribution that specifies the probability of each character occurring, independent of the positions. Finally, a hidden/latent variable is assumed that specifies the probability of a motif occurrence starting at each position in a given sequence.

Under such a model, motif extraction is formulated as a maximum likelihood estimation problem, and MEME uses an expectation-maximization (EM) based algorithm to maximize the expectation of the (joint) likelihood of the mixture model given both the data (sequences) and the latent variables. MEME uses a greedy search to find multiple motifs, where one motif is each “pass.” After each motif is discovered, information about the estimated parameters of the current motif’s model are incorporated back in to the mixture model. This prevents rediscovery of already identified motifs in future passes.

FASTA encoding. For processing via the MEME Suite, each sequence is first encoded in a proper format using the 24-character FASTA protein alphabet. To do this, we arbitrarily choose the first 18 non-ambiguous characters \mathcal{F} , and then specify a 1:1 mapping $\mathcal{S} \leftrightarrow \mathcal{F}$. We also only include sequences with $|\mathcal{S}| \geq 8$, which is the minimum allowable by MEME; there are 11,330 and 7,566 such sequences for ‘FMB’ and ‘NI’, respectively.

Running MEME. We input two files to MEME, one per course, to discover the motifs in the sequences. In running MEME, we set the number of unique motifs to search at 30, because this was seen to yield every motifs that had an E-value (*i.e.*, significance, discussed further below) less than 0.05. Also, we use the default background model of a 0-order Markov Chain. Through investigating each dataset, we observed that many sequences contained repeat subsequences; as a result, we used the motif model **and** that assumes that each sequence can obtain any number of non-overlapping occurrences of each motif. As for the EM algorithm, we chose the standard dirichlet prior based on the character frequencies, consistent with the background model.

With these parameters, we run MEME separately to discover motifs of different widths $w \in \{4, \dots, 10\}$. Other work has held the width constant, *e.g.*, at 4 in [17]. We choose this as the minimum size because anything below 4 is rather unspecific; on the other hand, we consider sizes up to 10 due to our more specific event set coding discussed in Sec. 2.2.1. A subset of the motifs discovered are shown in Fig. 6; there

⁵These standard quartiles will lead to interesting insights in Sec. 3. More generally, we can optimize the way the distributions are divided, which we leave for future work.

⁶The other events do not have this issue since they are not related to processing new information.

exist significant motifs at each endpoint of the range.

MEME output. For each motif, MEME gives (among other information) the E-value (E), and the position specific probability matrix (PSPM) describing the motif.

E-value: E indicates the significance of a motif. It is defined as the number of motifs (with the same width and occurrences) that would have equal or higher log likelihood ratio (LLR) if the sequences had been generated according to the background distribution. The LLR for a sequence is computed as $\log P(\text{seq}|\text{m}) - \log P(\text{seq}|\text{back})$, where the left term is the probability of observing the sequence (over all sightings) given the position-specific probabilities for the motif, and the right term is the probability of making this same observation under the background distribution.

PSPM: The PSPM of a motif gives the fraction of times that each character appears in each position of the motif, taken over all sightings of the motif in the dataset. In the following, denote the PSPM for a motif by $\mathbf{P} = [p_{ij}]$, where p_{ij} is the fraction of times event j occurs at position i .

Representation. At each position, we consider all events j with $p_{ij} \geq 0.25$.⁷ Formally, let \mathcal{A}_i be the sequence of indices into the event set \mathcal{S} for i , arranged such that $p_{i, \mathcal{A}_i(k)} \geq p_{i, \mathcal{A}_i(k+1)}$ and $p_{i, \mathcal{A}_i(k+1)} \geq 0.25$, $\forall k$. There are three cases on the way position i is represented:

- If $|\mathcal{A}_i| > 1$, i is represented as $[\mathcal{S}_{\mathcal{A}_i(1)} \mathcal{S}_{\mathcal{A}_i(2)} \dots]$.
- If $|\mathcal{A}_i| = 1$, then the square brackets are omitted, with just $\mathcal{S}_{\mathcal{A}_i}$ displayed.
- If $\mathcal{A}_i = \emptyset$, then i is displayed as ‘ \star ’ to indicate that this position was taken by a variety of events, none of which occurred even 25% of the time.

For example, the sequence [P12 P13] Pa1 \star [Sf1 Sf2 Sf4] is of length 4, with the first position being either P12 or P13 at least 50% of the time (P12 at least as often as P13), the second position being Pa1 at least 25% of the time, the third position being any event, and the last being either Sf, Sf2, or Sf3 at least 75% of the time.

Support. For each motif, we obtain the fraction of sequences (FS) in which it occurs, *i.e.*, its support, as well as the number of videos it appears in. To obtain this information, we use the MAST tool of the MEME Suite. This takes as input (i) a MEME output file describing the motifs and (ii) a sequence database in which to search for the motifs, and outputs the order and spacing of the motifs within each matching sequence. For MAST, a motif occurrence is defined as a position in the sequence whose match to the motif has a p-value less than $1\text{E-}4$.⁸

In order to see how the supports vary between correct and incorrect submissions, we apply this procedure for CFA and non-CFA sequences separately. Then, for each motif, the estimated probability of success \hat{p} (*i.e.*, of a CFA submission) related to a sequence containing this motif is $0.5 + \text{FS1} - \text{FS0}$, where FS1 and FS0 are the fraction of sequences in CFA and non-CFA for which the motif appears. In order to test whether \hat{p} is significant, we run a two-sample test

⁷With 18 different events, a threshold of 25% is roughly 5 times the expected occurrence from random selection.

⁸The p-value of a match is the probability of a random subsequence with the same length as the motif scoring at least as high as the match. To obtain the score, each motif is represented by its position-dependent scoring matrix, and the scores of the characters appearing at each position in the match are summed together.

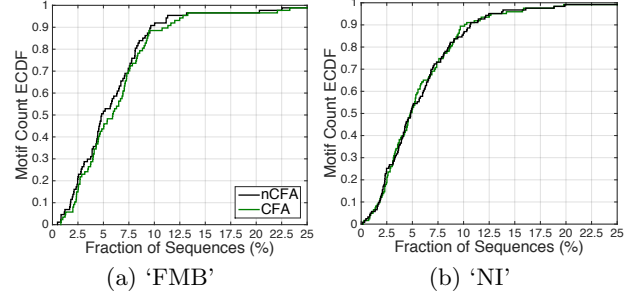


Figure 4: ECDFs of the number of sequences that each motif appears in, across both CFA and non-CFA. The supports are consistent across both groups.

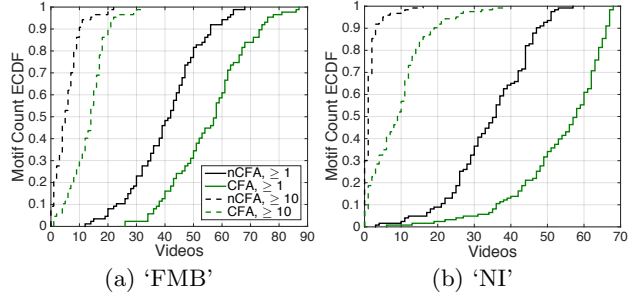


Figure 5: ECDFs of the number of videos that each motif appears in, across both CFA and non-CFA sequences. CFA sequences have a higher support for motifs across videos.

for proportions [16] for the null hypothesis that there is no difference between FS1 and FS0. If the p-value (p) for this test is low enough (≤ 0.05), then there is a large enough difference given the supports to conclude \hat{p} is significant.

3.2 Results

We obtained 87 and 123 motifs from ‘FMB’ and ‘NI’, respectively, which are the subject of the following analysis.

Motif overview. We first analyze how the motif supports vary across sequences and videos. Overall, we find that the motifs are reasonably supported across sequences and videos on average, for both CFA and non-CFA in each course.

Sequences: In Fig. 4, we plot the Empirical CDF (ECDF) of the fraction of sequences that each motif appears in, for both CFA and non-CFA. The supports are similar across these groups: for ‘FMB’, each motif appears in 5.9% of the non-CFA sequences on average, and 6.5% of the CFA; for ‘NI’, this is 5.8% for CFA, and 4.2% of the non-CFA. In both courses, the motifs with largest support (first row in Fig. 6(a) and (b)) appear in $> 25\%$ of the sequences.

Videos: Fig. 5 gives the ECDF of the number of videos that each motif occurred in at least once and at least 10 times. Here, CFA has higher support than non-CFA. We also see that the supports decrease for higher thresholds:⁹ For ‘FMB’ in (a), we can see that while the top 20% of the motifs appear in at least 67 videos for CFA (50 for non-CFA), this number is only 18 considering at least 10 occurrences (8 for non-CFA). For ‘NI’ in (b), the top 20% appear in at least 64 videos for CFA (44 for non-CFA), and this number drops to 14 for at least 10 occurrences (2 for non-CFA).

3.2.1 Individual motifs

⁹We see the same trends for thresholds besides 10 as well.

Group	Motif	E-value	FS	FS0	FS1	\hat{p}	p-value
Pa	I [P12 P13] [Pa4 Pa3] [P12 P11] [Pa2 Pa3] P12 Pa3 P12 [Pa2 Pa3] P13	5.3E-64	28.5	26.2	29.5	53.3	4.6E-4**
	II P12 Pa4 P12 Pa4	1.5E-06	13.2	13.2	13.3	50.1	0.901
	III [Pa1 Pa3] P11 [Pa2 Pa1] P11 [Pa1 Pa2] [P11 P12] [Pa1 Pa2] [P11 P12]	≈ 0	12.1	11.3	12.5	51.2	0.0745
	IV [P11 P13 P12] Pa4 P12 Pa3 [P12 P11] * P12 * [P13 P11] Pa3	1.5E-15	10.9	9.3	11.6	52.3	3.9E-4**
	V [P12 P11] Pa2 [P11 P12] Pa1 [P11 P12] Pa3 [P11 P12] Pa1 [P11 P12] Pa2	8.3E-109	9.27	9.65	9.10	49.5	0.374
Sb	I Sb3 [P12 P11] [Sb2 Sb3] P12 Sb2 P12 [Sb2 Sb3] [P13 P12]	6.0E-245	10.2	8.84	10.8	51.9	2.0E-3**
	II P13 Sb3 P12 [Sb3 Sb2] P13	6.7E-40	8.92	8.11	9.28	51.2	0.048*
	III P12 Sb2 [P11 P12] [Sb2 Sb3] P13	0.044	7.79	6.57	8.32	51.7	1.6E-3**
	IV [Sb2 Sb3] [P12 P11] Sb2 P12 [Sb2 Sb3] P12	1.6E-127	6.36	4.77	7.05	52.3	5.72E-06**
Sf	I P12 Sf3 [P11 P12] Sf2 [P11 P12] Sf1 [P12 P11] [Sf2 Sf1]	≈ 0	9.46	10.03	9.22	49.2	0.186
	II [P12 P11] [Sf2 Sf3] P11 [Sf3 Sf2]	≈ 0	6.42	7.41	5.98	48.6	4.95E-3**
Sf+Sb	I [Sf4 Sb4] [P11 P12] [Sf3 Sf4] [P11 P12] [Sf3 Sf4]	4.4E-104	7.41	8.08	7.11	49.0	0.0767
Sb+Pa	I [P12 P11] Sb2 P12 Sb2 [P12 P11] [Pa3 Sb2] P12 Pa2	3.2E-205	6.88	6.02	7.26	51.2	0.0177*
	II Pa3 [P12 P11] Pa2 [P11 P12] Sb2 [P12 P11] Sb2 [P12 P11] [Sb1 Pa2]	1.0E-38	6.85	6.36	7.06	50.7	0.191
Rf	I [P12 P13] Rf P12 Rf P13	8.0E-67	8.73	8.11	9.0	50.9	0.131
Rf+Rd	I P13 [Rf Rd] [P12 P11] Rf [P13 P12] Rf	≈ 0	4.55	3.89	4.84	50.9	0.0295*
	II Rf [P11 P12] Rd P13	2.3E-55	1.25	1.16	1.29	50.1	0.630
	III Rf Rd [P11 P12] Rf P13	1.2E-70	1.77	1.22	2.00	50.8	4.7E-3**
Rf+Sf	I [P11 P12] [Sf2 Rf] [P11 P12] Sf1 [P12 P11] [Sf2 Rf] P11 Sf1	≈ 0	1.94	1.80	2.00	50.2	0.523

(a) 19 Motifs for ‘FMB’.

Group	Motif	E-value	FS	FS0	FS1	\hat{p}	p-value
Pa	I [P12 P13] Pa4 [P12 P13] Pa4 P13	2E-81	26.8	27.6	26.5	48.8	0.338
	II P12 [Pa3 Pa4 Pa2] [P12 P11] [Pa3 Pa2] P12 [Pa3 Pa2]	2.2E-274	15.6	14.2	16.1	51.9	0.0529
	III P12 Pa4 P12 Pa4	1.8E-44	14.3	15.9	13.7	47.9	0.0233*
	IV P12 Pa4 P12 Pa3 P13	3.2E-19	11.8	11.0	12.1	51.0	0.241
	V P11 Pa1 P11 Pa1 P11 Pa1 [P11 P13]	≈ 0	11.7	12.7	11.4	48.7	0.145
Sb	I [Sb3 Sb4] [P12 P13] [Sb3 Sb2] P12 [Sb3 Sb2] [P13 P12]	9.1E-191	9.2	8.6	9.4	50.8	0.291
	II Sb3 P12 Sb2 [P12 P11] Sb2 P12 [Sb3 Sb2] [P13 P12]	2.2E-125	5.3	4.2	5.7	51.5	0.014*
Sf	I [P13 P11] [Sf3 Sf4] [P11 P12] [Sf4 Sf3 Sf2] [P11 P12] [Sf3 Sf4]	6.6E-100	7.8	8.9	7.4	48.4	0.0279*
	II P12 [Sf3 Sf2] P11 [Sf3 Sf2]	1.1E-248	7.7	9.7	7.0	47.4	2.2E-4**
Sb+Pa	I P13 [P13 P12] [Pa4 Pa3] Sb4 [P11 P12] Sb3 [P13 P12]	7.4E-26	10.9	11.6	10.6	49.0	0.247
	II [P12 P13] Pa4 P13 [Pa3 Sb4] [P12 P13] [Sb3 Sb4] [P12 P13] [Sb3 Pa4] P13	3.1E-28	7.6	6.5	8.0	51.5	0.0413*
	III Sb2 [P12 P11] [Sb2 Pa2] P12 [Sb2 Sb3] [P12 P13]	3.6E-108	5.7	4.8	6.1	51.3	0.0392*
Sf+Sb	I [Sb1 P12] Sf1 [Sb1 P11] [Sf2 Sf1] [Sb1 P11] [Sf1 Sf3] [Sb1 P12] [Sf1 Sf2]	≈ 0	9.0	10.1	8.6	48.5	0.0581
	II P12 Sf3 [P11 P12] [Sf3 Sf2] [P13 Sb1]	2.7E-3	6.3	7.2	6.0	48.8	0.0598
Rf+Rd	I [P11 Rd] Rf P11 Rf Rd [P11 P12] Rf P13	2.9E-177	3.9	4.6	3.6	49.0	0.0590
Rf+Pa	I [P11 P12] [Rf Pa1] P11 Rf [P11 P12] Rf [P11 P12] Rf [P12 P11] Rf	≈ 0	4.2	4.6	4.1	49.6	0.456
	II P11 Pa1 P11 [Pa1 Rf] P11 Pa1 P11 [Pa1 Rf] P11	≈ 0	8.2	7.6	8.5	50.9	0.254
Rf	I [P11 P12] Rf P12 Rf P12 Rf	≈ 0	9.1	9.4	9.1	49.6	0.665
	II Rf [P12 P11] Rf [P13 P12]	≈ 0	2.3	3.5	1.9	48.4	9E-5**
Rf+Rd+Rs	I [Rf Rs] [P12 P11] Rd [P12 P13] Rf	7.3E-16	2.5	3.1	2.3	49.2	0.064
Rf+Rd+Pa	I P11 [Rf Pa1] [P11 P12] Rf [Rd P11] Rf [Rf Pa1] [P11 P12] Rf [P13 P12]	3.8E-85	3.6	3.4	3.7	50.3	0.600

(b) 21 Motifs for ‘NI’.

Figure 6: Identified motifs for each course. Each motif is grouped by the events it contains outside of P1. FS is the fraction of sequences over both CFA and non-CFA, while FS0 and FS1 are for the separate cases. \hat{p} is the estimated probability of success (CFA) if a sequence contains the motif, and the p-value (p) is the significance of \hat{p} (* indicates $p \leq 0.05$, and ** is for $p \leq 0.01$). These motifs exhibit interesting behavioral patterns, some significantly associated with CFA or non-CFA.

We now analyze the most significant motifs, listed in Fig. 6. To generate this table, we applied the following procedure closely. First, noticing that all motifs contain P1 events, we group them into categories based on their other events, leading to 8 groups for ‘FMB’ and 10 for ‘NI’. Then, within each category, we consider each motif that either (i) has one of the top-10 highest supports or (ii) has a significant p (≤ 0.05) comparing CFA and non-CFA supports. Finally, if one motif is a subsequence of another and the relationship between CFA and non-CFA is the same for both, then we remove the one that has lower support or is less significant. This yields 19 and 21 motifs for ‘FMB’ and ‘NI’, respectively. Each of these is assigned an ID in Fig. 6 consisting of its group and number (e.g., Pa II is motif P12 Pa4 P12 Pa4). **Overview.** These motifs exhibit many similar structural attributes, which occur in spite of the fact that the encoding quantiles are different for each event and course (see Fig. 3). Also, since MEME finds ungapped motifs (i.e., those existing as exact matches in the data, without a separate layer of similarity matching), these identified behaviors exist

organically in the sequences, contrary to other work [17] which has resorted to approximate string searching. We find that the motif with highest support in each group tends to have the longest length (average of 7.5 over all groups with at least two motifs). Note also that the motifs in the Pa group have the largest supports (FS) overall ($\geq 10\%$ mostly), which is consistent with the fact that there are less skip and ratechange events in the datasets (see Fig. 3(b)). We present our most interesting observations for each group: **Reflecting (Pa).** The occurrence of play together with pause indicates that lectures are generally thought-provoking, causing students to *reflect on the material they just saw*. In both courses, the events forming the motifs in this group cover the entire range from short to medium-long plays (P11 – P13) interspersed with short to long pauses (Pa1 – Pa4).

The motif with the highest support in ‘FMB’ – Pa I – can be viewed as a long sequence of medium to medium-long plays followed by medium-long to long pauses, which is also characteristic of Pa IV in ‘FMB’. This behavior occurs more often in CFA class in both cases ($p \leq 0.01$). Motifs Pa III

and Pa V in ‘FMB’ as well as Pa V in ‘NI’ are long sequences too, but consist of short to medium plays followed by short to medium pauses and do not distinguish between CFA and non-CFA ($p > 0.07$). Motifs Pa II in ‘FMB’ and Pa I in ‘NI’ are also shorter sequences, but with medium to medium-long plays followed by long pauses, and also do not significantly differentiate between CFA and non-CFA ($p > 0.3$).

Note that in ‘NI’, the Pa group exhibits less discriminative capability. For this reason, we do not draw conclusions on differences between the classes from these sequences.

Revising (Sb, Sb+Pa). From the six motifs in the Sb group, we identify two interesting, recurring subsequences: P12 Sb3 P12 Sb3 (Sb I and II for ‘FMB’, and Sb I for ‘NI’), and P12 Sb2 P12 Sb2 (Sb III and IV for ‘FMB’ and Sb II for ‘NI’). Roughly speaking, each of these is associated with *playing for a length of video, and then revising some or all of that content*. To see this, consider the ranges of Pl and Sb from Fig. 3 associated with these subsequences: P12 covers 14 to 68 sec for ‘FMB’, and Sb2 to Sb3 covers 18 to 73 sec; for ‘NI’, these ranges are 12 to 71 sec and 13 to 55 sec. The play and skip ranges are closely overlapping in each case. Taking the extreme ends of each range, they are associated with skipping back anywhere from 1 min below the starting play point to 50 sec after it,¹⁰ which are local considering the video lengths. This is further justified by the fact that Sb4, a long skipback, does not appear in these subsequences. Note that 5 of the 6 motifs containing these behaviors are significantly associated with CFA ($p \leq 0.01$).

We also considered the number of skip backs originating at each video position across all UV Pairs. We find that the largest origination point of these events is at the end of the video. In particular, out of all Sb events, those originating within 10 sec of the videos’ end constitute 16% and 13% of the total for non-CFA and CFA in ‘FMB’.¹¹ This, combined with the motifs suggesting revision when Sb occurs, implies that those students who are revising *multiple times* before answering a quiz have a higher chance of success.

Consistent with the observation for Sb, 4/5 of the motifs in Sb+Pa are significantly associated with CFA ($p \leq 0.02$). **Skimming (Sf, Sf+Sb).** In both of the courses, the motifs in the Sf group are primarily medium to long skips forward with short to medium plays in-between. Further, the skips are longer than the plays occurring before and after; comparing the lengths of Pl and Sf events in Fig. 3, we see that for both courses, range Q_j to Q_{j+1} for Sf is always larger than Q_{j-1} to Q_j for Pl. This recurring behavior in the Sf group can then be interpreted as *skimming through the material quickly* with less exposure to the material. We find that 3 of these 4 motifs are significant in favor of non-CFA ($p \leq 0.03$). We contrast this to a finding in [6], where the total number of skip forwards in a sequence was not found to be significantly associated with either CFA or non-CFA. This underscores the utility of considering the clickstream sequences, rather than computing aggregate quantities to summarize them.

While Sb+Sf can possibly be interpreted as *skipping forward with caution*, we find that this is also close to being significant in favor of non-CFA ($p < 0.06$).

Speeding. Referring to Rf+Rd in ‘FMB’, motifs I and III

indicate that viewing the material at a faster than default rate, *i.e.*, *speeding*, is more often associated with the CFA class than not ($p < 0.03$). With these motifs, learners also return to the default rate, indicating they are *slowing down for important content*. To this point, in ‘FMB’, we see no significant motifs for slower than default rates; however, one does exist in ‘NI’ (Rf+Rd+Rs). Also, Rf II in ‘NI’ is more significantly associated with non-CFA ($p = 9E-5$), which could indicate that a faster rate is harmful in this course.¹²

3.2.2 Key messages

Overall, we make a few conclusions from our analysis:

Reflecting. Pausing to reflect on material repeatedly is the most commonly recurring behavior. If the time spent reflecting is not *too* long, but longer than the time spent watching, then a positive outcome is most likely (in ‘FMB’).

Revising. Repeated revision of the material suggests students will gain a better understanding of the content.

Skimming. Skimming through material quickly, even with caution, is costly in terms of knowledge gained.

Speeding. Students who watch the videos at a faster than default rate may already be familiar with the material, leading to a correct answer (in ‘FMB’). They also may slow to the default if they sense unfamiliar material.

Based on these conclusions, we emphasize the importance of having included the lengths, in addition to the events, in this framework. As an example, the sequence P1 Sb P1 Sb identified in [17] cannot be associated with revising, because it is not clear how far back the student has skipped relative to having played. In the same way, P1 Sf P1 Sf cannot be concluded as skimming.

From these findings, it is clear that clickstream motifs are useful in studying behavior, and that they can be significantly related to performance. In terms of using them to model behavior for CFA prediction, however, there are two drawbacks. First, while the supports are reasonable considering these are rather long subsequences, none of the motifs appear in a majority of the sequences (max 28.5%). Second, none of the \hat{p} success estimates deviate substantially from 50% (max 3.3%). Hence, we will now turn to an alternate clickstream sequence representation which is more applicable to CFA prediction. Nonetheless, some of the conclusions made from this analysis will guide our modeling choices.

4. MODEL OF POSITION SEQUENCE

In this section, we will formalize a position-based sequence representation, which factors in the location in the videos that a student visited. Then, we will preset CFA models based on this framework, which will be evaluated in Sec. 5.

4.1 Modeling Framework

We begin with a few definitions. Let $v \in \mathcal{V}$ denote video v in the set of videos \mathcal{V} for a course, indexed chronologically (*i.e.*, by release date of the videos).¹³ Also, let $c \in \mathcal{C}$ denote class c in the set of binary classes $\mathcal{C} = \{0, 1\}$, where $c = 0$ indicates a non-CFA submission and $c = 1$ is CFA. With $u \in \mathcal{U}$ as user u in the set of all users \mathcal{U} , we let $\mathcal{U}^v \subset \mathcal{U}$ be the set of users who have a UV Pair for v , and $\mathcal{U}^{v,c} \subset \mathcal{U}^v$ be those

¹⁰We assume a default playback rate as an approximation.

¹¹As a reference point, if we take the maximum location of Sb origination for each video outside of the last 10 sec, these constitute 4.5% and 3.6% of the total for non-CFA and CFA.

¹²It is worth mentioning that the instructor of ‘NI’ tends to deliver content at a quicker pace than in ‘FMB’.

¹³Recall from Sec. 2.1 that we consider a “video” to be all videos for a given quiz.

who fall into class c with respect to their answer submission. For evaluation in Sec. 5, we will generate training (\mathcal{U}_T^v) and test (\mathcal{U}_E^v) sets as subsets of \mathcal{U}^v through a procedure described in [6]; \mathcal{U}_T^v and \mathcal{U}_E^v are always chosen such that $\mathcal{U}_T^v \cap \mathcal{U}_E^v = \emptyset$.

4.1.1 Position-based sequence specification

We divide each video into a number of intervals. Let h_v be the length (in sec) of v . We define w_v to be the width that partitions v into $N(w_v) = \lfloor h_v/w_v \rfloor$ uniform intervals, such that interval $i \in \mathcal{P}^v(w_v) = \{1, \dots, N(w_v)\}$ spans the range $[(i-1) \cdot w_v, i \cdot w_v]$.¹⁴ For each UV Pair, we can then model the behavior as a sequence of positions $\mathbf{p}^{u,v} = (\rho_1, \rho_2, \dots, \rho_n, \dots)$, where $\rho_n \in \mathcal{P}^v(w_v)$ is the index of the n th position visited.¹⁵

In generating these positions, we first apply the same denoising procedure described in Sec. 2.2.1 to each event E_i . Then, for each UV Pair, we do the following, starting with \mathbf{p} as an empty sequence:

1. For E_1 , add $\lfloor p_1/w_v \rfloor$ to \mathbf{p} .
2. Consider each sequential pair of events E_i, E_{i+1} , $i \geq 1$. If $s_i = \text{paused}$, then only $\lfloor p_{i+1}/w_v \rfloor$ is added to \mathbf{p} . But if $s_i = \text{playing}$, then:
 - If $e_i \neq \text{Skip}$, then $\lfloor p_i/w_v \rfloor + 1, \dots, \lfloor p_{i+1}/w_v \rfloor - 1, \lfloor p_{i+1}/w_v \rfloor$ is added to \mathbf{p} .
 - If $e_i = \text{Skip}$, then the addition to \mathbf{p} is instead $\lfloor p_i/w_v \rfloor + 1, \dots, \lfloor p'_i/w_v \rfloor - 1, \lfloor p'_i/w_v \rfloor, \lfloor p_{i+1}/w_v \rfloor$.¹⁶

For example, suppose $h_v = 300$, $w_v = 15$, and a user generates $E_1 = \langle \text{Play}, 0, 0, \text{playing}, 1.0 \rangle$, $E_2 = \langle \text{skip}, 200, 50, \text{playing}, 1.0 \rangle$, $E_3 = \langle \text{ratechange}, 230, 80, \text{playing}, 1.25 \rangle$, and $E_4 = \langle \text{pause}, 300, 127, \text{paused}, 1.25 \rangle$ on the video. Then, $\mathbf{p} = (0, 1, 2, 3, 13, 14, 15, 15, 16, \dots, 20)$.

4.1.2 Model factors

In general, there are (at least) three types of information for each $\mathbf{p}^{u,v}$ that could have an effect on performance:

Positions. The number of times a given ρ_i was visited. One would expect these to be different between CFA and non-CFA, because certain parts of the videos will be more important to the questions than others. To see this, we can refer to two types of motifs which were identified as associated with CFA: *reflecting*, which indicates that these sequences may have more visits to important positions through pausing, and *revising*, which suggests that these sequences may have more visits to positions associated with the questions through repeated revision before answering the question. Further, the *skimming* motif suggests that non-CFA sequences will have less visits to important positions.

Transitions. The number of transitions between the positions, *i.e.*, the number of times ρ_i, ρ_j is a subsequence of $\mathbf{p}^{u,v}$, across each pair i, j . This is related to the type of event that was executed between i and j :

- If $\rho_j < \rho_i$, then the user had skipped back. We call this a *backward* transition.
- If $\rho_j > \rho_i + 1$, then the user had skipped over the material in (p_i, p_j) . We call this a *forward* transition.

¹⁴We choose the last interval to be of variable size extending to the end of the video.

¹⁵For brevity, we will typically refer to $\mathbf{p}^{u,v}$ as just \mathbf{p} , with the understanding that it refers to the UV Pair in question.

¹⁶Recall from Sec. 2.2.1 that when E_i is a skip event, p'_i is the position of the video player immediately before the skip.

- If $\rho_j = \rho_i + 1$, then the user moved directly to the next position. This is a *direct* transition.
- If $\rho_j = \rho_i$, then the user had some event *within* the current position. This is a *repeat* transition.

We say that direct and repeat transitions are *local*, whereas backward and forward are *non-local*. As with positions, the transition factors can capture the motif behavior, but in terms of sequences of visits.

Time spent. The amount of time spent at the different positions. One would expect these times to be discriminatory in a similar manner to visit frequencies.

In order to evaluate the benefit of including each of these factors, we will consider four prediction models: Discrete time Positions (DP), which incorporates the number of visits to each position; Continuous time Positions (CP), which uses the time spent at each position; Discrete time Transitions (DT), which models transitions between positions; and Continuous time Transitions (CT), which factors in inter-arrival times between positions. Each of these models are trained on each video separately, which allows us to compare prediction quality on a per-video basis in Sec. 5.

4.2 Position Models

For the DP and CP models, video positions are treated as independent events.

4.2.1 Discrete Time Positions (DP)

Let $\mathbf{f}^{v,c} = [f_i]^{v,c} \in [0, 1]^{N(w_v)}$ be the probability distribution of visit frequency across positions $i \in \mathcal{P}^v(w_v)$. This is estimated over the UV Pairs in the training set $\mathcal{U}_T^{v,c}$ as

$$f_i^{v,c} = O_i^{v,c} / \sum_j O_j^{v,c}, \quad (1)$$

where $O_i^{v,c}$ is the number of occurrences of p_i over sequences in $\mathcal{U}_T^{v,c}$, *i.e.*, $O_i^{v,c} = \sum_{u \in \mathcal{U}_T^{v,c}} \sum_n \mathbb{I}_{\{\rho_n = i\}}$.

We test the ability of this model to identify which class each $u \in \mathcal{U}_E^v$ belongs to. For this purpose, we compute the likelihood of observing \mathbf{p} on video v to be in c , given $\mathbf{f}^{v,c}$, as

$$L(\mathbf{p} | \mathbf{f}^{v,c}) = g^{v,c} \cdot \prod_n f_{\rho_n}^{v,c}, \quad (2)$$

where $g^{v,c} = |\mathcal{U}_T^{v,c}|/|\mathcal{U}_T^v|$ is the estimated class bias for video v . Then, the prediction $\tilde{c} \in \{0, 1\}$ of the class for \mathbf{p} is determined by application of the Maximum a Posteriori (MAP) decision rule. But recall that there is a bias towards $c = 1$ for each course (see Fig. 1). As a result, we introduce a term $b_v \geq 0$ into MAP, which will be tuned through the cross validation procedure described in Sec. 5.1:

$$\tilde{c} = \begin{cases} 1 & L(\mathbf{p} | \mathbf{f}^{v,1}) > L(\mathbf{p} | \mathbf{f}^{v,0}) + b_v \\ 0 & L(\mathbf{p} | \mathbf{f}^{v,1}) < L(\mathbf{p} | \mathbf{f}^{v,0}) + b_v \\ \mathbb{I}_{\{U \geq g^{v,0}\}} & \text{otherwise} \end{cases}, \quad (3)$$

where U denotes a random number drawn from $[0, 1]$.

4.2.2 Continuous Time Positions (CP)

In this model, we consider the holding times within each position. Let $\mathbf{r}^{v,c} = [r_i]^{v,c} \in \mathcal{R}^{N(w_v)}$ be the vector of the total time spent by $\mathcal{U}_T^{v,c}$ in state i . This is estimated as

$$r_i^{v,c} = \sum_{u \in \mathcal{U}_T^{v,c}} \sum_n \mathbb{I}_{\{\rho_n = i\}} \cdot d_n, \quad (4)$$

where d_n is the duration of event n in \mathbf{p} (see Sec. 2.2.1).

We will assume that the holding times at each position are exponentially distributed. The reason for this is to have a direct comparison with the CT model in Sec. 4.3, where the interarrival times also have this distribution. The estimates in (4) then become the means of the distributions, and the likelihood of \mathbf{p} for a UV Pair in \mathcal{U}_E^v is

$$L(\mathbf{p} | \mathbf{r}^{v,c}) = g^{v,c} \cdot \prod_i (1/r_i^{v,c}) \exp(-T_i/r_i^{v,c}), \quad (5)$$

where

$$T_i = \sum_n \mathbb{I}_{\{\rho_n=i\}} \cdot d_n \quad (6)$$

is the total time spent by sequence \mathbf{p} at position i .

The MAP for CP is the same as (3), except substituting (5) for (2).

4.3 Transition Models

In modeling transitions between positions, we will only consider one-step transitions. This is common in webpage clickstream analysis (e.g., [22]), and will be useful here since the state spaces we consider can be large, depending on w_v .¹⁷

4.3.1 Aggregating non-local transitions

The cohort estimator for a Markov Chain model uses the fraction of transitions from state i to j in estimating the probability of transitioning from i to j [14]. We found this model not appropriate here, because the number of transitions between two non-local positions is rather sparse, implying that there is not enough data to estimate these specific transitions.

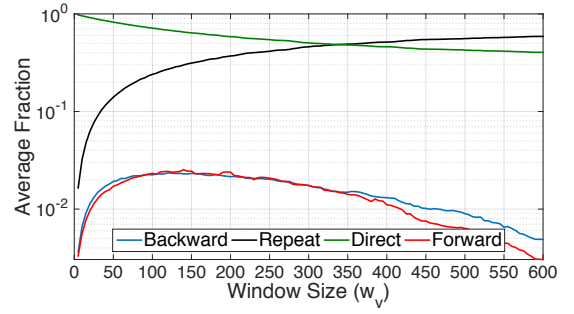
To see this, we inspect the $\mathbf{p}^{v,c}$ for varying w_v . For each position in video v , we find the total number of the four types of transitions across the UV pairs, aggregate these over all positions, and then find the fraction of each type of transition. We do this for all $w_v \in \{5, 10, \dots, 600\}$ (i.e., through 10 min), and then average across the videos v for each w_v . Fig. 7 shows the result; we make two observations: *Tradeoff between local transitions*: As w_v increases, the percentage of repeat transitions increases monotonically (1.7% to 59% for FMB, 2.8% to 58% for NI), while the percentage of direct transitions decreases monotonically (98% to 40% for FMB, 97% to 41% for NI). This is to be expected, since each position is increasing in size with w_v , and hence the next event is more likely to be in the current window.

Infrequent non-local transitions: The vast majority of transitions are *local*, i.e., either repeat or direct. In particular, from Fig. 7, the largest fraction of backward transitions is 2.3% ($w_v = 120$) for ‘FMB’ and 1.5% for ‘NI’ ($w_v = 60$), and that for forward transitions is 2.4% (for $w_v = 150$) for ‘FMB’ and 1.2% for ‘NI’ ($w_v = 70$).

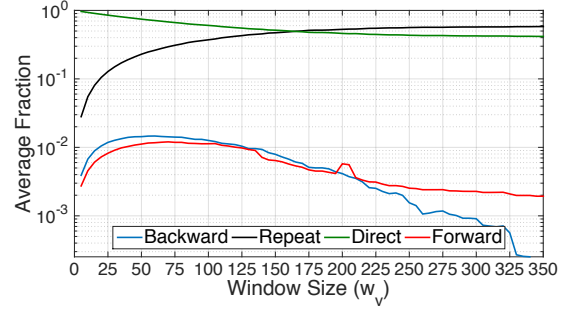
As a result, our models will aggregate all observed forward transitions to form a single, uniform probability at each position, and likewise for backward. To this end, we define

$$\mathcal{I}_{i,k} = \begin{cases} \{1, \dots, i-1\}, & k=1 \\ \{i\}, & k=2 \\ \{i+1\}, & k=3 \\ \{i+2, \dots\} & k=4 \end{cases}$$

¹⁷This may not be ideal because unlike sequences of webpages, learning builds on itself. It is harder to estimate higher order transitions due to position-specific data sparsity. We still see substantial benefit with a one-step model.



(a) ‘FMB’



(b) ‘NI’

Figure 7: Plot of the fraction of local (repeat and direct) and non-local (backward and forward) transitions for each window size w_v , averaged over all UV Pairs for each position and video v , for each dataset. Clearly, the fraction of non-local transitions is very low in each case, reaching a maximum of 2.4% for forward transitions in ‘FMB’ (at $w_v = 150$).

to be the set of states constituting a backward ($k=1$), repeat ($k=2$), direct ($k=3$), and forward ($k=4$) transition at position i .

4.3.2 Discrete Time Transitions (DT)

In this model, we discretize time, discounting the interarrival times. Let $\mathbf{F}^{v,c} = [f_{i,k}^{v,c}]^{v,c} \in [0, 1]^{N(w_v), 4}$ be the matrix of transition probabilities, where $f_{i,k}^{v,c}$ is the probability that the next position will be in $\mathcal{I}_{i,k}$ given the current is i . We also assume that the transitions are homogeneous, i.e., independent of time n .

Considering the sequences of positions \mathbf{p} across users $u \in \mathcal{U}_T^{v,c}$, we obtain the number transitions from i to k as

$$O_{i,k}^{v,c} = \sum_{u \in \mathcal{U}_T^{v,c}} \sum_n \mathbb{I}_{\{\rho_n=i, \rho_{n+1} \in \mathcal{I}_{i,k}\}}.$$

From this, we estimate the $f_{i,k}^{v,c}$ as

$$f_{i,k}^{v,c} = O_{i,k}^{v,c} / \sum_j O_{i,j}^{v,c}, \quad (7)$$

and the likelihood of \mathbf{p} from user $u \in \mathcal{U}_E^v$ on video v is

$$L(\mathbf{p} | \mathbf{F}^{v,c}) = g^{v,c} \cdot f_{\rho_1}^{v,c} \cdot \prod_n f_{\rho_n, \rho_{n+1}}^{v,c}, \quad (8)$$

where $f_{\rho_1}^{v,c}$ is the distribution at the initial position ρ_1 of \mathbf{p} , obtained from (1). The MAP for DT is again the same as in (3), except with (8) in place of (2).

4.3.3 Continuous Time Transitions (CT)

This model incorporates the interarrival times between transitions. Rather than computing the time-varying tran-

	w_v		b_v		Acc		F1	
	avg	s.d.	avg	s.d.	avg	s.d.	avg	s.d.
SKR	-	-	-	-	0.56	0.07	0.63	0.11
DP	206	152	1.3E-6	6.2E-6	0.64	0.08	0.73	0.12
DT	297	165	1.3E-6	6.2E-6	0.64	0.08	0.69	0.16
CP	355	226	0.04	0.20	0.57	0.07	0.61	0.17
CT	198	138	8.8E-8	2.70E-7	0.64	0.08	0.72	0.15

(a) ‘FMB’

	w_v		b_v		Acc		F1	
	avg	s.d.	avg	s.d.	avg	s.d.	avg	s.d.
SKR	-	-	-	-	0.58	0.08	0.67	0.12
DP	106	68	9.9E-5	2.9E-4	0.66	0.10	0.74	0.18
DT	121	87	1.1E-3	5.5E-3	0.65	0.10	0.73	0.15
CP	328	182	0.03	0.18	0.59	0.08	0.66	0.16
CT	88	68	5.6E-6	3.0E-5	0.66	0.10	0.74	0.17

(b) ‘NI’

Figure 8: Summary of the tuned parameters window size (w_v) and likelihood bias (b_v), and the performance metrics accuracy (Acc) and F1 obtained across the video groups for each course.

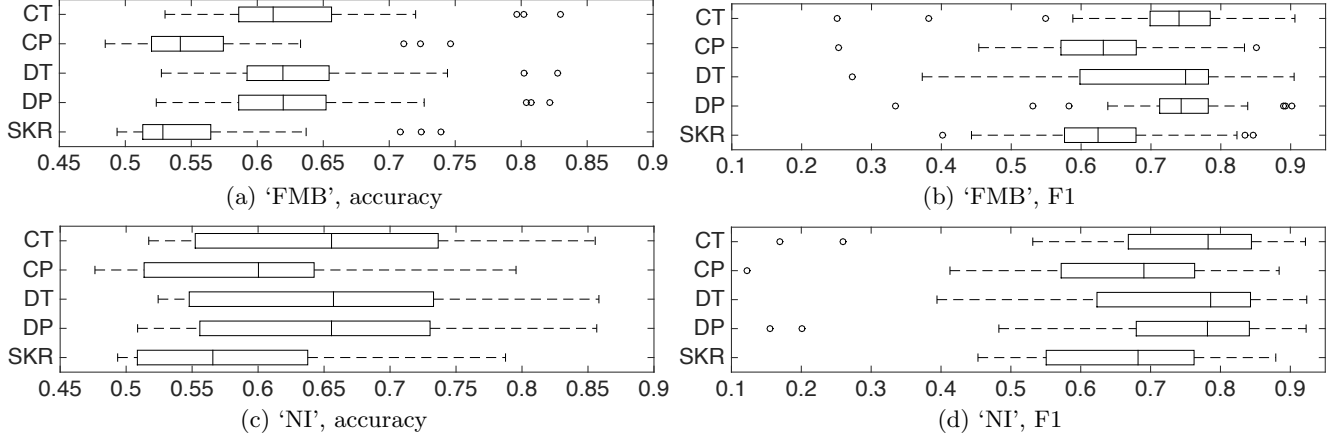


Figure 9: Boxplots of CFA prediction performance across both courses, considering accuracy and F1. Here, each datapoint is the obtained performance on one of the videos considered. Overall, we see that DP, DT, and CT outperform SKR for both metrics, and especially for accuracy, while CP performs comparable to SKR.

sition probabilities, we instead work with the transition rates [14]. To this end, let $\mathbf{Q}^{v,c} = [q_{i,k}]^{v,c} \in \mathcal{R}^{N(w_v),4}$ be the transition rate matrix for the model, where $q_{i,k}$, $k \neq 2$ represents the rate of departure from position i and arrival at a position in $\mathcal{I}_{i,k}$. In estimating the $q_{i,k}$, we first obtain the number of transitions from i to k over users $u \in \mathcal{U}_T^v$ as

$$O_{i,k}^{v,c} = \sum_{u \in \mathcal{U}_T^{v,c}} \sum_n \mathbb{I}_{\{\rho_n = i, \rho_{n+1} \in \mathcal{I}_{i,k}\}}, \quad k \neq 2.$$

Then, the $q_{i,k}^{v,c}$ terms are computed as

$$q_{i,k}^{v,c} = \begin{cases} O_{i,k}^{v,c} / r_i^{v,c} & k \neq 2 \\ -\sum_{k \neq 2} q_{i,k}^{v,c} & k = 2 \end{cases}, \quad (9)$$

where $r_i^{v,c}$ is the total time spent in i , defined in (4). From this, the likelihood of sequence \mathbf{p} for $u \in \Omega_E^v$ is obtained:

$$L(\mathbf{p} | \mathbf{Q}^{v,c}) = g^{v,c} \cdot \prod_{i,k;k \neq 2} (q_{i,k}^{v,c})^{o_{i,k}} \exp(-q_{i,k}^{v,c} \cdot T_i), \quad (10)$$

where T_i is the time spent by \mathbf{p} in i , as defined in (6), and $o_{i,k} = \sum_n \mathbb{I}_{\{\rho_n = i, \rho_{n+1} \in \mathcal{I}_{i,k}\}}$, $k \neq 2$ is the number of transitions from i to k for the sequence \mathbf{p} . Once again, MAP is as in (3), except with (10) in place of (2).

5. PREDICTION EVALUATION

In this section, we evaluate the performance of the models described in Section 4. We pose the following questions:

1. How beneficial is it to include positions and transitions for CFA prediction on individual videos?
2. Is one of position or transition-based model clearly better than the other, or would some combination be the best?

3. Is it beneficial to include position durations?

Skewed-Random (SKR). In our investigation, we also consider one algorithm that does not make use of clickstream data, to act as a baseline for comparison [6]. It finds the CFA bias $g^{v,1}$ over $\mathcal{U}_T^{v,1}$, and predicts $c = 1 \cdot g^{v,1}$ of the time.

5.1 Procedure

Metrics. Let TP, FP, TN, and FN be the number of true and false positives, and true and false negatives obtained by a model through evaluation over \mathcal{U}_E^v . In selecting the model parameters w_v and b_v over \mathcal{U}_T^v , we choose those leading to highest accuracy, *i.e.*, $(TP + TN)/(TP + FP + TN + FN)$. Since the quizzes are biased towards CFA (see Fig. 3), we found that unconstrained maximization of accuracy led to parameters with high recall (rec), *i.e.*, $TP/(TP + FN)$ but low precision (prec), *i.e.*, $TP/(TP + FP)$. To avoid this, we subject the search to the constraint that the chosen parameters have at least 25% of the truly negative samples predicted negative, and likewise for the positives, averaged over the training evaluations. To this end, we will also consider the standard (balanced) F1 score for each model, obtained as $2 \cdot (\text{prec} + \text{rec})/(\text{prec} + \text{rec})$. As the harmonic mean of prec and rec, F1 is limited by the minimum of the two.

Cross Validation (CV). As stated in Sec. 4.1, \mathcal{U}_T^v and \mathcal{U}_E^v are always chosen such that $\mathcal{U}_T^v \cap \mathcal{U}_E^v = \emptyset$. To do this, we divide \mathcal{U}^v into K -folds $\mathcal{U}_1^v, \mathcal{U}_2^v, \dots, \mathcal{U}_K^v$, and average the results of training the model on $\mathcal{U}_T^v = \mathcal{U}^v \setminus \mathcal{U}_j$ and testing the model on $\mathcal{U}_E^v = \mathcal{U}_j$ for $j \in \{1, \dots, K\}$. This K -fold CV process is repeated N times, and the results averaged over the N trials. In generating $\mathcal{U}_k^v \forall k$, we ensure that the number of positive and negative samples is consistent across each fold. To do this, for each CV iteration we randomly allocate $|\mathcal{U}^{v,0}|/K$

	SKR	DP	DT	CP	CT		SKR	DP	DT	CP	CT
SKR	—	1.1E-4**	7.9E-5**	0.56	1.2E-4**	SKR	—	1.9E-3**	0.044*	0.99	4.0E-3**
DP	1.1E-4**	—	0.86	2.1E-4**	0.83	DP	1.9E-3**	—	0.78	1.8E-3**	0.88
DT	7.9E-5**	0.86	—	2.3E-4**	0.67	DT	0.044*	0.78	—	0.030*	0.98
CP	0.56	2.1E-4**	2.3E-4**	—	2.5E-4**	CP	0.99	1.8E-3**	0.030*	—	4.3E-3**
CT	1.2E-4**	0.83	0.67	2.5E-4**	—	CT	4.0E-3**	0.88	0.98	4.3E-3**	—
(a) FMB, accuracy						(b) FMB, F1					
	SKR	DP	DT	CP	CT		SKR	DP	DT	CP	CT
SKR	—	2.0E-3**	2.7E-3**	0.61	1.2E-3**	SKR	—	3.3E-3*	0.022*	0.95	2.3E-3**
DP	2.0E-3**	—	1	8.0E-3**	0.85	DP	3.3E-3*	—	0.81	4.9E-3**	0.94
DT	2.7E-3**	1	—	0.012*	0.87	DT	0.022*	0.81	—	0.026*	0.64
CP	0.61	8.0E-3**	0.012*	—	4.3E-3*	CP	0.95	4.9E-3**	0.026*	—	3.6E-3**
CT	1.2E-3**	0.85	0.87	4.3E-3*	—	CT	2.3E-3**	0.94	0.64	3.6E-3**	—
(c) NI, accuracy						(d) NI, F1					

Figure 10: p-values from applying pairwise WRS tests to the boxplots in Fig. 9. A * indicates significance at a confidence level of 0.05, and ** at 0.01.

elements from $\mathcal{U}^{v,0}$ and $|\mathcal{U}^{v,1}|/K$ elements from $\mathcal{U}^{v,1}$ into \mathcal{U}_k^v (without replacement). For our experiments, we set $N = 10$ and $K = 5$, for a total of 50 runs in each CV iteration.

Parameter tuning. Each algorithm has two parameters that must be tuned: the video width w_v , and the likelihood bias b_v . We treat both of these as discrete parameters, with a fine granularity of search. In particular, in each CV iteration, we choose a different pair $(w_v, b_v) \in \{5, 10, \dots, 20, 30, 45, \dots, 600\} \times \{0, 2^{-60}, 2^{-57.5}, \dots, 1\}$, for a total of 182 iterations for each v . In the end, we select the combination which yields the highest accuracy, subject to the constraint stated above. For w_v , we choose this set of values since (i) 5 sec corresponds to the threshold of combining repeat events (see Sec. 2.2.1), and (ii) 600 is close to the minimum video length in both courses. For both parameters, these choices were seen to ensure that most selections across videos did not lie on one of the grid endpoints.

5.2 Results and Discussion

After tuning, we evaluate each algorithm through CV. Since there is a sharp dropoff in quiz participation over time, we only consider those for which there are at least 100 samples of both CFA and non-CFA classes, so that there at least 20 samples from each class in each of the 5 CV folds. This leaves a total of 24 videos for ‘FMB’ and 32 for ‘NI’.

Overview of results. Summary information on the tuned w_v and b_v values, as well as the two performance metrics – Accuracy and F1 – can be found for each course in Fig. 8, where we give the mean and s.d. across the tested videos. We expect the performance to be higher for accuracy than for F1 score, because we chose parameters based on this metric through tuning. The distribution of the performance values across videos are plotted for each course in Fig. 9; in each box, the performance on one video is one data point. Additionally, the percent improvement relative to SKR for each video is shown in Fig. 11 for ‘FMB’ and in Fig. 12 for ‘NI’.

From Fig. 9, we can see immediately that the DP, DT, and CT algorithms perform the best overall, and that CP is comparable to SKR.¹⁸ A larger window has a denoising effect, because it aggregates more information within each

position and transition; the fact that CP chooses the largest window size on average in both courses (over 5.5 min) is an indication that the holding times alone can be noisy.

In order to test for significance in the performance differences between each pair of models, we run a WRS test [16] for the null hypothesis that there is no difference between the distributions in Fig. 9.¹⁹ The resulting p-values (p) are tabulated in Fig. 10, and verify the observed differences.

1: Benefit of clickstream data. We assess how beneficial the position and transition information is for prediction.

Accuracy: Considering accuracy first, we refer to Fig. 9(a&c). Here, we see that the DP, DT, and CT models are clearly shifted to the right relative to SKR, indicating higher quality. This difference is also statistically significant for each algorithm across both courses ($p \leq 2.0E-3$). For both ‘FMB’ and ‘NI’, the average improvement of these three algorithms relative to SKR is roughly 14% in each case. Further, referring to Fig. 11&12(a), we see that each algorithm outperforms SKR in each individual video. CP, on the other hand, only has a slight edge over SKR, with an average improvement of less than 2% for each course.

F1: For F1, we refer to Fig. 9(b&c). Again, we see that DP, DT, and CT are shifted to the right relative to SKR overall, but not as substantially. This is especially true for DT, which has a high range of F1 scores (0.63 and 0.53 for ‘FMB’ and ‘NI’ excluding outliers). For DP and CT, the average improvements in F1 of roughly 16% for ‘FMB’ and 10% for ‘NI’ are again significant ($p \leq 4.0E-3$); for DP, the differences of roughly 9% for both courses are also significant but not as substantially ($p \leq 0.04$). In Fig. 11&12(b), we see that for individual videos, DP and CT both outperform SKR in roughly 90% of the cases; for DT, 76% for ‘FMB’ and 88% for ‘NI’. CP performs roughly the same as SKR, with the average slightly lower.

We remark that there are a total of four videos (indexes 5 and 17 in ‘FMB’, 3 and 27 in ‘NI’) where most of the DP, DT, CP, and CT algorithms perform *substantially worse* than SKR in terms of F1. These videos also correspond to the outliers observed below the first quartiles in Fig. 9(b&d). One would expect that these would be instances where SKR already had high performance due to a high bias in favor of CFA. Surprisingly, the opposite is true here: SKR performance is within 0.01 of 0.5 in three of the cases, and within

¹⁸It is possible that CP would perform better under a different probability distribution assumption in Sec. 4.2, though CT had significant improvement with the same assumption. In future work, we will consider other distributions for CP.

¹⁹Again, we use the WRS test because Shapiro-Wilk tests detected significant departures from normality.

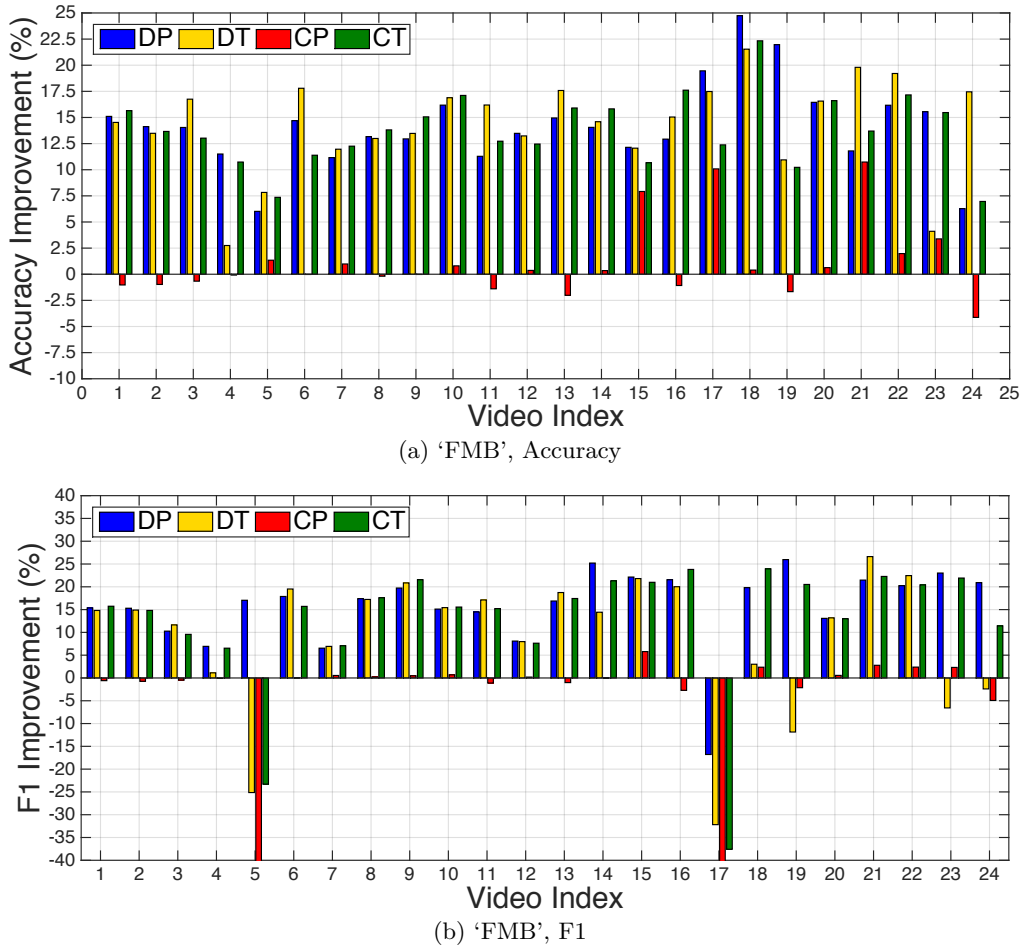


Figure 11: Percent improvements of each algorithm relative to SKR in ‘FMB’, for each of the videos. For Accuracy in (a), we see that the DP, DT, and CT algorithms outperform SKR in all cases. For F1 in (b), at least one of these algorithms outperforms SKR in all cases except 5 and 17.

0.03 in all of them. But there are also cases of SKR having performance in this near-random range, *i.e.*, with the videos having biases near 0.5, where the other algorithms do outperform SKR substantially.

2: Positions vs. transitions. We compare DP to DT, and CP to CT, case by case.

DP vs. DT: In terms of accuracy, DP and DT are comparable for both courses. As for F1, DP has modestly better performance, especially for ‘FMB’ where it has an improvement over DT of roughly 6%. Additionally, the lower quartiles for DT are shifted to the left relative to DP. When considering individual videos, however, the results are more mixed: for each course, DT and DP each perform better in roughly 50% of the cases. Overall, the differences between DT and DP are not statistically significant ($p \geq 0.78$).

CP vs. CT: CT is superior to DP for each metric and dataset, with the results significant in all cases ($p \leq 4.3E-3$).

3: Discrete vs. continuous. Finally, we compare discrete to continuous. For brevity, we only present CT and DT (since CT outperforms CP). In terms of accuracy, both algorithms are comparable. As to F1, CT is modestly better for ‘FMB’, with an improvement of roughly 4%. However, the differences are not statistically significant. CT outperforms DT in half of videos for ‘FMB’, and 59% for ‘NI’.

Key messages. Many aspects of position-based video behavior are useful for CFA prediction: the frequency of visits

to each position (DP), the frequency of transitions between positions (DT), and transitions incorporating holding times (CT). These benefits are also measured on individual videos, which underscores the applicability of these models to situations where there is not a lot of information across multiple lectures, *e.g.*, for quick detection early in a course. The holding times alone (CP), however, were seen to be too noisy. Both positions and transitions can be useful; DP, DT, and CT are comparable overall, performing better on different sets of videos, suggesting an ensemble may work best.

6. RELATED WORK

We discuss recent, key works on MOOC, and student video-watching analysis and CFA prediction.

MOOC studies. With the proliferation of MOOC in recent years, there have been a number of analytical studies on these platforms. Some have focused on a more general analysis of all learning modes, *e.g.*, [2, 12] studied learner engagement variation over time and across courses. Others have focused on specific modes. In terms of forums, [7] analyzed the decline in participation over 73 courses. In terms of assessments, [9] focused on predicting assignment completion in MOOC. Our work is fundamentally different from these in that it explores the *association* between behavior with two modes: videos and assessments.

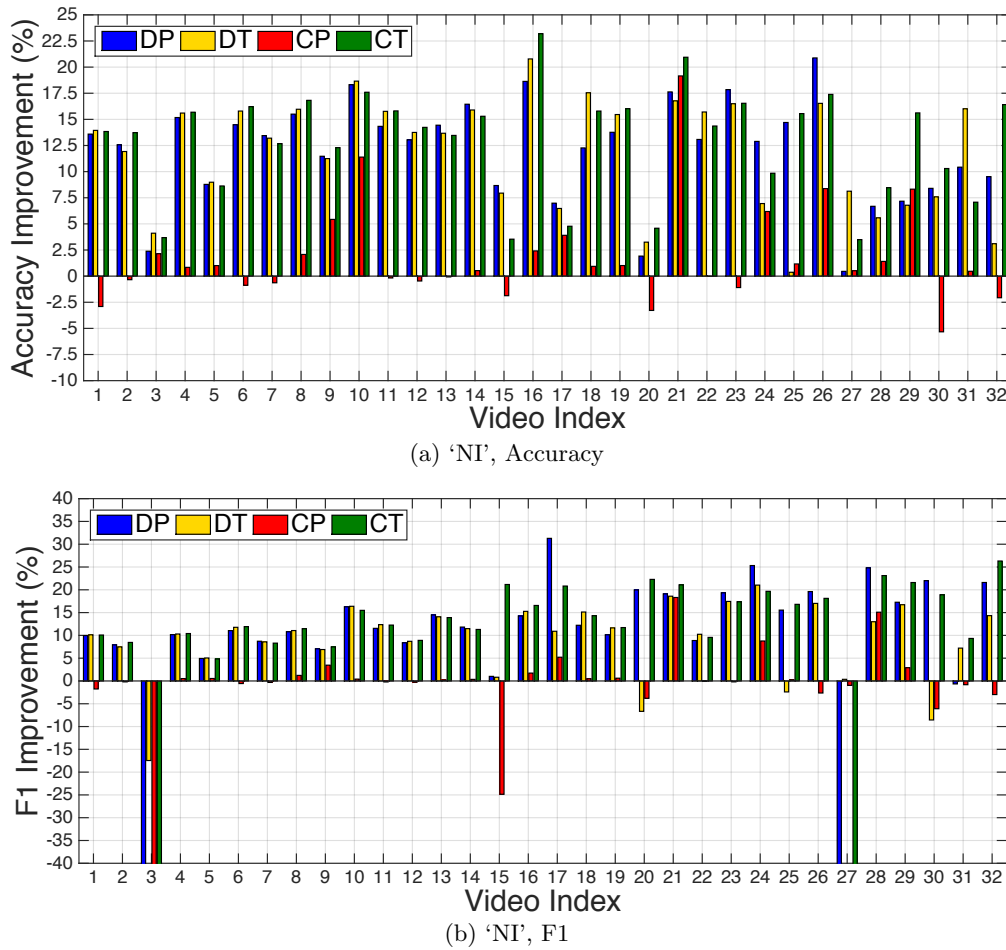


Figure 12: Percent improvements of each algorithm relative to SKR in 'NI', for each of the videos. The findings are qualitatively similar to those for 'FMB' in Fig. 11; for Accuracy in (a), DP, DT, and CT outperform SKR in all cases, and for F1 in (b), at least one of them outperforms SKR in all cases except two (3 and 27).

Video-watching analysis. Much existing work studying learner video-watching behavior [11, 6] has focused session-level user characteristics (*e.g.*, rewatching sessions), rather than click-level information. The work in [17] is most similar to ours, since it is also concerned with recurring patterns in clickstream sequences for MOOC users. The authors define a mapping of subsequences of events to predefined behavioral actions (*e.g.*, skipping, slow watching) and perform approximate string search to locate these behaviors in clickstreams. From these actions, they devise a scheme to infer a learner's Information Processing Index (IPI), which is in turn predict engagement, next click, and dropout of students. Our work on motif identification differs in two important ways: (i) rather than assuming a predefined set of behavioral actions, we extract the most prominent motifs using motif identification algorithms, and (ii) we are concerned with mapping motifs to efficacy, whereas in [17] the objective is to predict engagement, next click, and dropout.

[18] also studies video-watching clickstreams, except the sequences they define include events from both videos and forums (*e.g.*, play and pause on the video, as well as post and comment on the forums). In this way, they are focused on a more complete view of the learner experience, including transitions both within and across these different learning modes. Also, the short work in [1] presents the possibility of representing video clickstream trajectories as a time se-

ries of playback position over real (UNIX) time for a single video used in a FLIP course, as opposed to the sequence of events approach. Analysis in this way opens the possibility of applying time series similarity methods (*e.g.*, dynamic time warping) to further compare watching behavior.

Performance prediction. Researchers have developed predictors for whether a student will be CFA or not on a question in traditional education settings. Collaborative filtering (CoF) algorithms have been applied as classification models for this purpose (*e.g.*, [21, 4]). Others have probabilistic graphical models (PGMs) [15], when there is coarse-granular information collected (*e.g.*, course difficulty) over multiple sessions. Recently, [13] developed SPARFA-Trace, a framework for learner and content analytics which traces a learner's knowledge evolution through the sequence of material he/she has accessed and assessments he/she answered. Compared with these works, ours is unique in that (i) it focuses instead on relating click-level behavioral data – video-watching behavior – to performance, and (ii) it focuses on prediction within single videos.

In general, there has been a lack of work on CFA prediction for MOOC, where the fraction of assessments a user completes can be much less due to participation dropout [7]. The recent work of [6] studied the predictive capability of session-level video-watching quantities computed from clickstream data (*e.g.*, the fraction of the video watched and the

number of rewinds), considering multiple users and videos in the course simultaneously. Focusing on individual videos, our models are instead position-dependent, and the improvements in accuracy relative to the baseline that we obtain are strictly higher than those cited here (14% vs. 9.5% max).

Webpage clickstream analysis. Clickstream analysis for user webpage browsing behavior remains an active area of research [22, 10, 19]. For example, [19] focused on extracting palindromes present in clickstream sequences, and related these to analytics for web optimization. Video-watching clickstreams are fundamentally different than these applications, which concern transitions between webpages rather than behavior within a single window.

7. CONCLUSION

In this work, we studied student video-watching behavior, performance, and their association in MOOC. In doing so, we formalized two frameworks for representing user clickstreams: one based on sequences of events with discretized lengths, and one based on sequences of positions visited. With datasets from two MOOCs encoded in these frameworks, we accomplished two goals: (1) we mined the sequences to identify recurring motifs in user behavior, and discovered that some of these characteristics are significantly associated with CFA and non-CFA quiz submissions; (2) we proposed models for relating user clickstreams to knowledge gained, and showed how multiple aspects of this behavior can improve CFA prediction quality on individual videos.

There are a number of next steps we are investigating, *e.g.*, to use the identified motifs for user and content analytics; to optimize the selection of quantiles used divide the event lengths based on the resultant motifs; to consider position durations under a non-exponential assumption; and to see whether prediction improvement can be obtained through higher order transitions.

8. REFERENCES

- [1] J. M. Aiken, S.-Y. Lin, S. S. Douglas, E. F. Greco, B. D. Thoms, M. D. Caballero, and M. F. Schatz. Student use of a single lecture video in a flipped introductory mechanics course. *arXiv:1407.2620*, 2014.
- [2] A. Anderson, D. Huttenlocher, J. Kleinberg, and J. Leskovec. Engaging with massive online courses. In *Proceedings of the 23rd international conference on World wide web*, pages 687–698. International World Wide Web Conferences Steering Committee, 2014.
- [3] T. L. Bailey, M. Boden, F. A. Buske, M. Frith, C. E. Grant, L. Clementi, J. Ren, W. W. Li, and W. S. Noble. Meme suite: tools for motif discovery and searching. *Nucleic acids research*, page gkp335, 2009.
- [4] Y. Bergner, S. Droschler, G. Kortemeyer, S. Rayyan, D. Seaton, and D. E. Pritchard. Model-based collaborative filtering analysis of student response data: Machine-learning item response theory. In *Proceedings of the 5th International Conference on Educational Data Mining*, pages 95–102. ERIC, 2012.
- [5] C. G. Brinton and M. Chiang. Social learning networks: A brief survey. In *48th IEEE CISS*, pages 1–6. IEEE, 2014.
- [6] C. G. Brinton and M. Chiang. Mooc performance prediction via clickstream data and social learning networks. In *To appear, 34th IEEE INFOCOM*. IEEE, 2015.
- [7] C. G. Brinton, M. Chiang, S. Jain, H. Lam, Z. Liu, and F. M. F. Wong. Learning about social learning in moocs: From statistical analysis to generative model. *IEEE Trans. Learning Technol.*, 7:346–359, 2014.
- [8] C. G. Brinton, R. Rill, S. Ha, M. Chiang, R. Smith, and W. Ju. Individualization for education at scale: Miic design and preliminary evaluation. *IEEE Trans. Learning Technol.*, 8(1), 2015.
- [9] J. Cheng, C. Kulkarni, and S. Klemmer. Tools for predicting drop-off in large online classes. In *Proceedings of the 2013 conference on Computer supported cooperative work companion*, pages 121–124. ACM, 2013.
- [10] S. Gündüz and M. T. Özsu. A web page prediction model based on click-stream tree representation of user behavior. In *9th ACM SIGKDD*, pages 535–540. ACM, 2003.
- [11] J. Kim, P. J. Guo, D. T. Seaton, P. Mitros, K. Z. Gajos, and R. C. Miller. Understanding in-video dropouts and interaction peaks inonline lecture videos. In *L@S*, pages 31–40. ACM, 2014.
- [12] R. F. Kizilcec, C. Piech, and E. Schneider. Deconstructing disengagement: analyzing learner subpopulations in massive open online courses. In *Proceedings of the third international conference on learning analytics and knowledge*, pages 170–179. ACM, 2013.
- [13] A. S. Lan, C. Studer, and R. G. Baraniuk. Time-varying learning and content analytics via sparse factor analysis. In *20th ACM SIGKDD*, pages 452–461. ACM, 2014.
- [14] J. R. Norris. *Markov chains*. Number 2. Cambridge university press, 1998.
- [15] Z. Pardos and N. Heffernan. Using hmms and bagged decision trees to leverage rich features of user and skill from an intelligent tutoring system dataset. *Journal of Machine Learning Research*, 2011.
- [16] D. J. Sheskin. *Handbook of parametric and nonparametric statistical procedures*. crc Press, 2003.
- [17] T. Sinha, P. Jermann, N. Li, and P. Dillenbourg. Your click decides your fate: Inferring information processing and attrition behavior from mooc video clickstream interactions. In *2014 EMNLP*, 2014.
- [18] T. Sinha, N. Li, P. Jermann, and P. Dillenbourg. Capturing attrition intensifying structural traits from didactic interaction sequences of mooc learners. *EMNLP 2014*, page 42, 2014.
- [19] M. Speiser, G. Antonini, A. Labbi, and J. Sutanto. On nested palindromes in clickstream data. In *18th ACM SIGKDD*, pages 1460–1468. ACM, 2012.
- [20] K. Stephens-Martinez, M. A. Hearst, and A. Fox. Monitoring moocs: which information sources do instructors value? In *Proceedings of the first ACM conference on Learning@ scale*, pages 79–88. ACM, 2014.
- [21] A. Toscher and M. Jahrer. Collaborative filtering applied to educational data mining. *KDD Cup*, 2010.
- [22] G. Wang, T. Konolige, C. Wilson, X. Wang, H. Zheng, and B. Y. Zhao. You are how you click: Clickstream

analysis for sybil detection. In *USENIX Security*, pages 241–256, 2013.